SIMULTANEOUS MEASUREMENTS OF THE PLANAR VELOCITY AND TEMPERATURE STRUCTURE FOR THE CHARACTERIZATION OF FLAMES

by

*DIETER MOST, MATHIAS RAISCH, FRIEDRICH DINKELACKER AND ALFRED LEIPERTZ*

Department of Technical Thermodynamics
University Erlangen-Nürnberg
Am Weichselgarten 8, 91058 Erlangen, Germany

ABSTRACT

For modeling purposes of turbulent premixed flames, detailed information about the flow $\leftrightarrow$ flame interaction is extremely interesting. Thereby, the turbulent flow field is mainly characterized by spatial structures, gradients and vortices, inducing local flow divergencies and strain rates. This process influences the local transport and reaction processes in the flame front. Due to the spatial and stochastic nature of turbulent structures, correlated measurements of the spatial temperature field and the spatial velocity field are of great value.

With the recently developed planar filtered Rayleigh scattering (FRS) technique, for measuring the temperature field, and simultaneous application of particle image velocimetry (PIV), combined 2D information about the instantaneous velocity field and the temperature structure of the flame is achievable. From that data, vortical flow structures can be determined directly conditioned to the local flame conditions. Here, the advancement of the planar laser Rayleigh scattering for the filtering technique of FRS allows the suppression of otherwise interfering Mie scattering from the tracer particles, which are necessary for PIV measurements. Details of FRS technique and its simultaneous application with PIV are described in the paper.

First experiments have been performed on two turbulent premixed flames, a weak turbulent V-flame and a highly turbulent bluff-body stabilized burner. Some examples of simultaneously obtained flow field and temperature field data are discussed. Additionally, comparisons have been done between conditioned and non-conditioned determination of the mean velocity, the velocity fluctuation and of the mean turbulent strain rate, including also a time-averaged evaluation of these parameters from LDV data. The comparison reveals that correct determination of turbulent flow parameters in the flame brush is only reasonable for temperature conditioned evaluation, as can be done with this new proposed FRS-PIV technique. If determination of the mean strain rate is performed non-conditioned, this results in significantly biased (too high) values.
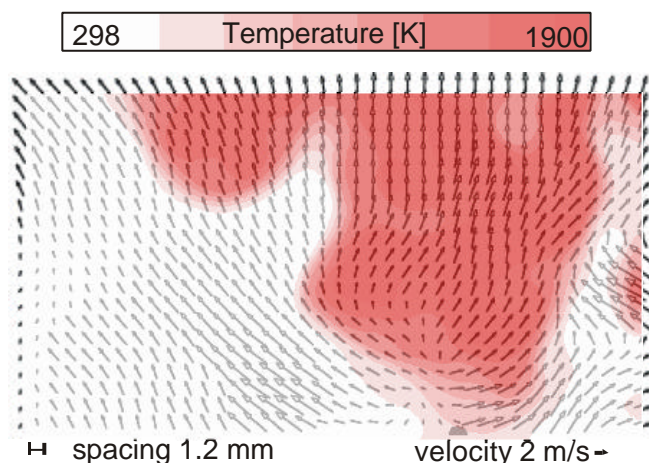
Instantaneous velocity and temperature field of a V-Flame

1 INTRODUCTION

Turbulent flow fields are determined by their transient local gradients and vortices. Dependent on the scale, the scale distribution and the strength of thee properties the burning behavior of turbulent flames can be influenced in different ways altering the transport processes between cold unburnt and hot burnt gases. For premixed flames visible effects of altered reactions are generally observed for flame conditions which are located in the traditional Borghi-diagram proposed by Peters (1986) in the regime of the "distributed reaction zone". Investigations of flames at these conditions have produced different, sometimes contradictory results. While O'Young, et al. (1997) determined a thickening of the flame front others [Most, et al. (1999), Soika, et al. (1998)] measure a thinning of the front and again others [Mansour, et al. (1998)] observed a modified pre-heat zone with still intact thin reaction zone. Roberts, et al. (1992), Bradley (1992) and also Poinsot, et al. (1993) determined quenching and local extinction due to flame $\leftrightarrow$ vortex interaction. Recently Dinkelacker, et al. (1998) observed the above mentioned effects in highly turbulent flames to happen simultaneously, indicating that for the wide statistical distribution of velocity parameters in turbulent flow field also a wide distribution of alternating burning conditions are existing for one flame. This indicates that conditional two dimensional measurements of local velocity and reaction parameters are necessary to obtain accurate information of the local flame-flow interaction in highly turbulent flows.

On the other hand premixed-flames have small characteristic length scales, thus only non-intrusive optical techniques are applicable to measure flow and flame processes without alteration. To measure flow properties two techniques have been established, laser Doppler velocimetry (LDV) and particle image velocimetry (PIV) While the first one provides point measurements along a time axis, only from PIV two dimensional data of cross sections of 2 velocity components can be obtained instantaneously. Thus a simultaneous application of PIV with techniques, resolving the flame front structures, would provide more detailed insight of the local flow-flame interaction.

For flames some combined investigations, mainly from simultaneous PIV and LIF techniques [e.g., Frank, et al. (1999), Rehm, et al. (1998); Carter, et al. (1998)] have been published. Thereby laser induced fluorescence (LIF) provides data about intermediate products like OH and CH. But since the OH radical will be produced first above 1200 K and CH is only visible in the reaction zone closely to 1500 K no information about the temperature structure of the pre-heat zone can be obtained from that approach. Here, light sheet tomography (LST) [Stevens, et al. (1998)], which determines the density of the seeding particles from Mie scattering might be suitable technique for obtaining temperature information simultaneously. But for that a constant seeding density has to be achieved to correlate the particle and the gas density, which is, e.g., in a highly turbulent bluff-body burner not possible. Considering only the applicability of 2d temperature measurements in flames, planar laser Rayleigh scattering (LRS) might be usable [Most, et al. (1999), Soika, et al. (1998)]. Unfortunately due to problems of LRS with Mie scattering from particles, which eclipses the Rayleigh signal, combined measurements have only been performed with LDV techniques [Duarte, et al. (1995)], using an anti-discrimination method. But instantaneous 2d correlation of flow eddies with the flame temperature distribution have not been possible yet.

A new, very promising approach, which overcomes the disadvantage of LRS of being sensible to interfering Mie scattering, is to use the recently developed filtered Rayleigh scattering technique (FRS) [Hofman, et al. (1996), Forkey (1996), Elliott, et al. (1996)]. Here, the simultaneous measurement of velocity field (via PIV) and temperature field (via FRS) is possible and has recently proved to obtain suitable results [Most, et al. (2000)].

From these combined data now a determination of the instantaneous velocity field (and also of derived quantities like strain rates) conditioned to the temperature structure of the flame can be deduced. Thus the potential is given for a more detailed investigation of the influence of the local flow field on the flame front structure. Now traditional flow parameters for a classification of the flow conditions can be achieved locally at the flame front and be correlated directly the flame. First measurements in this direction are presented in this paper for two different premixed methane/air flames, a wire stabilized flame and a bluff-body burner. From that the extension of the evaluation technique for critical parameters to temperature conditioned determination is shown to be reasonable.
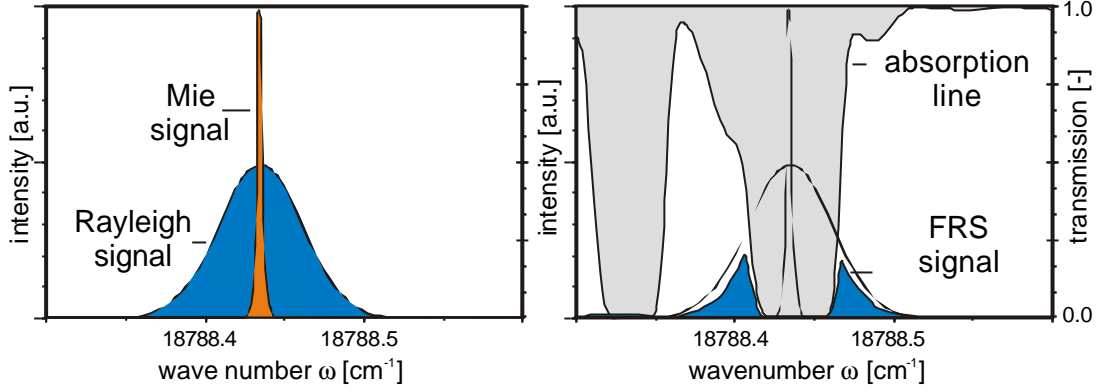
Fig. 1:   Schematic of the obtained spectra from Rayleigh and Mie scattering at 532 nm (left) and of the FRS signal, filtered by an absorption line of iodine vapor as ultra-thin notch filter (right).

2   MEASUREMENT TECHNIQUE

2.1   Filtered Rayleigh Scattering

Filtered Rayleigh scattering technique (FRS) [Hofman, et al. (1996), Most, et al. (1999), Most, et al. (2000)] is an extension of the conventional LRS technique, which tolerates a certain amount of Mie-scattering and expands the possibilities of applying Rayleigh scattering techniques on conditions, where additional Mie scattering takes place. FRS is no longer limited on pure gaseous media without scattering surfaces from particles and fixtures and therefore enables the 2d measurement of temperature in flow fields loaded with particles. Thus, it also provides the possibility of applying FRS simultaneously with measurement techniques using Mie scattering as a signal source, e.g., the particle image velocimetry (PIV).

The main idea of FRS is to use the fast and statistically distributed thermal movement of molecules, causing large Doppler broadening, to separate the Rayleigh signal from Mie signals, which are only slightly broadened for particles and surfaces with low velocities (Ma<1). If stimulated now by narrow band light, a very thin notch filter can block the Mie signal and the center of the Rayleigh signal completely while information from the flanks of the broadened Rayleigh signals is not affected and can still be detected (compare Fig. 1). But contrary to the LRS technique, where the scattering cross section factors are nearly constant with temperature, now the cross section factor depends on the spectral broadening, and thus on the thermodynamic state of the investigated gas sample. Modeling of the scattering spectra is necessary. For diluted gases (kinetic scattering regime) the molecules are isolated scattering centers and therefore the spectra can be calculated as a superposition of the individual molecules of the gas sample. With lower temperatures and higher pressures (hydrodynamic regime), Brillouin scattering occurs. Here molecule interactions, e.g. collisions and density or entropy fluctuations have to be considered additionally and the scattering spectra is no longer a simple superposition of individual scattering processes.

For practical determination of the temperature in a flame a similar approach as for the conventional LRS technique [Leipertz, et al. (1992)] is used. For every pixel (x,y) the integral over the measured the filtered signal $I(\lambda_0)$ has to be compared with that of a reference state $I_{ref}(\varpi)$ (here air at 25 °C,1 bar), which is obtained for the same optical setup, laser intensities I_0 and incident wavelength λ_0:

$$\left(\frac{I(\lambda_0)}{I_{ref}(\lambda_0)} \right)_{x,y} = \left(\frac{N}{N_{ref}} \cdot \frac{\sigma_{FRS}(\lambda_0)}{\sigma_{FRS,ref}(\lambda_0)} \right)_{x,y} \qquad (1)$$

Thus unknown setup constants, e.g. aperture or local laser intensity can be canceled. The ratio of the signals $I(\lambda_0)/I_{ref}(\lambda_0)$ is now a function only of the ratio of molecule number N/N_{ref} in the sample volume and the alteration of the scattering cross section factors $\sigma_{FRS}(\lambda_0)/\sigma_{FRS\ ref}(\lambda_0)$ for the filtered signal. If $\sigma_{FRS}(\lambda_0)/\sigma_{FRS\ ref}(\lambda_0)$ is known, from N/N_{ref} by considering the ideal gas law the temperature can easily be deduced. For application the measured temperature is deduced by comparing the measured ratio $I(\lambda_0)/I_{ref}(\lambda_0)|_{meas}$ with a simulated ratio $I(\lambda_0)/I_{ref}(\lambda_0)|_{sim}$ being a function of temperature and gas composition.

For modeling purposes of $\sigma_{FRS}(\lambda_0)$ for atmospheric methane/air flames the kinetic scattering mechanism can be assumed for all temperatures (<273 K), accepting a small error for cold gases since the fuel mixture at environment temperature is located in the transition regime between kinetic and hydrodynamic regime. For increased temperatures the gas composition of this flame is completely located in the kinetic scattering regime.

The kinetic scattering model is based on Doppler effects of independent scattering centers. For every molecule and every temperature the Gaussian shaped thermal velocity distribution and from that their spectral distribution $S_{kin,i}(k,\varpi)$ due to Doppler shift to the incident light can be calculated [Chu (1991)]:

$$S_{kin,i}(k,\varpi) = \left[(2\pi)^{0.5}/kv_0 \right] \exp\left(-\varpi^2/2k^2 v_0^2 \right) \qquad (2)$$

In eq. (2) $k = 4\cdot\pi\cdot\sin(\theta/2)/\lambda_0$ represents the incident wave vector with the angle θ between k and observation direction and $\varpi = (\omega_0-\omega)$ the relative shift to the incident wave number ω_0. The average molecule velocity v_0 is calculated from temperature T, Boltzmann constant k_B and the mass of the molecule m_i to:

$$v_0 = \sqrt{\frac{k_B T}{m_i}} \qquad (3)$$

Then the relative FRS scattering cross section $\sigma_{FRS,i}$ results from integration over the scattered spectra $S_{kin,i}$ (T, k,ϖ), multiplied with the filter function of the vapor cell T(ϖ). After scaling with the respectively Rayleigh scattering cross section $\sigma_{Ray,i}$ and division by the integral over the unfiltered $S_{kin,i}$ (T, k, ϖ), the FRS cross section factor results:

$$\sigma_{FRS,i} = \frac{\sigma_{Ray,i}}{\int S_{kin,i}(T,k,\varpi)d\varpi} \cdot \int \left(T(\varpi) \cdot S_{kin,i}(T,k,\varpi) \right) d\varpi \qquad (4)$$

Thereby the absorption spectra T(ϖ) of the molecular filter cell has to be modeled, too. For the here used iodine vapor cell filled T(ϖ) can be calculated from algorithms proposed by Forkey, et al. (1997).

By definition, collisions between molecules do not have to be considered in the kinetic regime. Thus the average FRS cross section for a gas mixture can be calculated as superposition of the independent scattering parts, of every component:

$$\overline{\sigma}_{FRS}\big|_{kin} = \sum_i c_i \cdot \sigma_{FRS,i}\big|_{kin} \qquad (5)$$

Assuming the concentrations c_i in the flames to be a known function of temperature, the composition of the gas mixture can be calculated for every T (e.g., here from CHEMKIN calculations for laminar flames). Then the ratio $I(\lambda_0)/I_{ref}(\lambda_0)$ can be determined for every temperature.

2.2 Particle image velocimetry

With PIV the motion of tracer particles in the flow is measured. If the particles are small enough (ideal tracers) their motion represents also the gas flow velocity. Since PIV itself is a well established technique for standard flow systems, only a short introduction is given here. For more detailed information about PIV techniques, e.g., Raffel, et al. (1998) or IoP (1997) is recommended.

For the 'classical form' of PIV these particles are mapped onto a camera two times in short time intervals, e.g., being illuminated by two laser pulses. Then from the displacement of the particles two velocity components of the flow can be obtained in the plane of the laser light sheet. By imaging on two separate pictures cross correlation techniques are used for data evaluation. Here, the image is subdivided into a grid of small raster elements, containing several particles. For the displacement of each of these elements one vector is determined. Thus for every point of the grid one flow vector - for oversampling a respectively higher number – is obtained. From the flow field data further flow properties, e.g. local strain components and the vorticity can be calculated.
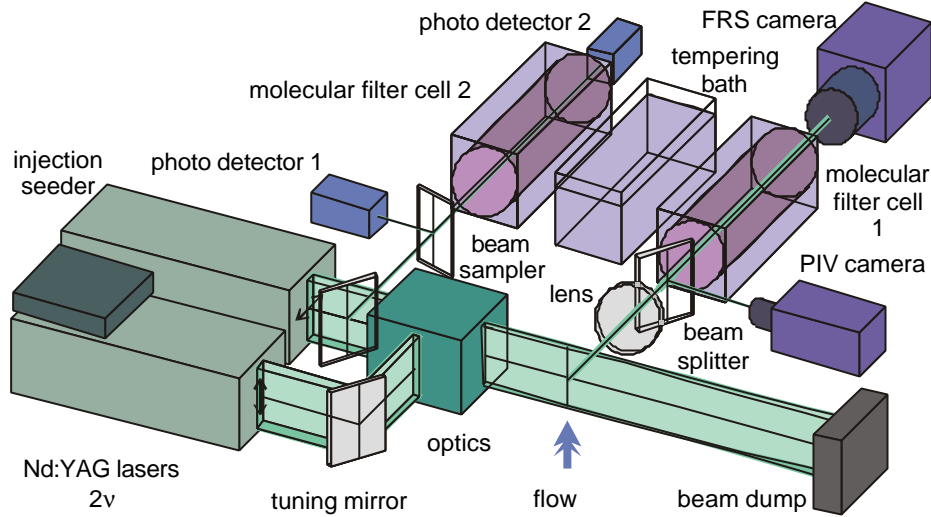
Fig. 2:   Setup for simultaneous application of filtered Rayleigh scattering thermometry (FRS) and particle image velocimetry (PIV)

3   EXPERIMENTAL APPROACH FOR SIMULTANEOUS MEASUREMENT

3.1 - Particle image velocimetry

Experimental Setup

Two serial pulses from two separate Nd:YAG lasers (532 nm) are superposed by an polarizing beam splitter to a light sheet which is used to create a cross section through the investigated flame (Fig. 2). The scattered light is collected by a spherical lens and divided in two equal parts (PIV and FRS signal) by a non-polarizing beam splitter. The PIV signal is imaged on a 12 bit CCD camera with double shutter option (1280x1024, PCO). Thus two short-time separated ($\Delta t \sim 30\,\mu s$) images of the particles are obtained. A laser-line band path filter (532 nm, not shown in Fig. 2) is used to suppress chemiluminescene of the flame.

Data evaluation

After binarising the images on a suitable threshold, the velocity vectors are determined from those image pairs using cross correlation techniques (VISIFLOW). From that for each raster element (32x32 pixels; 50 % oversampling) one velocity vector $\vec{v}$ is calculated. Thus from a initial camera resolution of about $37\cdot37\,\mu m^2$ per pixels a vector separation of $\sim 600\,\mu m$ results.

From the vector field data further flow parameters can be achieved. From the 2d velocity field data only the z component of the vorticity can be calculated to [Raffel, et al. (1998)]:

$$w = \nabla \times \vec{v}_{x,y,z} \rightarrow w_z = \frac{\partial v_y}{\partial x} - \frac{\partial v_x}{\partial y} \qquad (6)$$

Also the local shear strain rate ε_{xy} can be determined for every raster element:

$$\varepsilon_{xy} = \frac{\partial v_x}{\partial y} + \frac{\partial v_y}{\partial x} \qquad (7)$$

3.2 Filtered Rayleigh scattering

Experimental Setup

For simultaneous application of FRS thermometry with PIV, one of the above mentioned lasers is operated with an injection seeder to obtain a tunable single mode pulse at 532 nm. Then the wavelength is tuned to an absorption line of molecular iodine vapor, which is used as an optically thin notch pass filter. Thereby the superposition of wavelength and absorption line is monitored by two photodiodes and a second filter cell. The FRS signal itself is imaged by an ICCD camera passing the first vapor cell and a laser-line bandpath filter (532 nm). By adjusting the temperature of the body of the cell to 30°C±0.5 °C (tempering bath), the filter cell (pure I_2; length 41 cm) is operated in the two phase regime (solid-gaseous). Condensation of solid iodine at the optical windows is suppressed by keeping their temperature slightly above T_{cell}. Thus the vapor pressure of iodine is linked to the temperature T_{cell} of the cell body. The obtained pixel resolution is about 176·176 µm².

Data evaluation

To reduce noise and eliminate residual fractions from the Mie scattering of the particles, the raw image data of FRS is purified with a series of median filters (3x3, 5x5, 7x7). From the measured reference picture at known thermodynamic state (air, 25°C, 1 bar) an average reference image I_{ref} is calculated. Then each single-shot image of the flame is divided by $I_{ref}(x,y)$. Finally, the temperature is determined by comparing the ratio $I(\lambda_0)/I_{ref}(\lambda_0)|_{x,y}$ with modeled data for every pixel of every single-shot image. Thereby the absorption spectra $T(\varpi)$ of the molecular filter cells filled with iodine vapor can be calculated from algorithms proposed by Forkey, et al. (1997).

3.3 Investigated flame types

For experiments two turbulent premixed methane/air flame types have been investigated. The first one is a less turbulent wire stabilized V-flame, the second one is from a highly-turbulent bluff-body burner. For this flame types former experiments have been are already presented [Soika, et al. (1998); Most, et al. (1999)]. Both configurations have been investigated systematically for equivalence ratios $\phi = 0.6$-0.8 and exit velocities $v_{exit} = 5.7$-8.5 m/s for the bluff-body configuration, respectively $v_{exit} = 0.90$-1.35 m/s for the V-flame.

The bluff-body burner consists of a nozzle (d = 0.048 m), in which a bluff-body (d = 0.044 m) can be placed concentrically. 0.1 m upstream of the nozzle a turbulence grid (plate; 48 holes with d = 0.002 m) ensures isotropic incoming flow of the bluff-body. Thus the nozzle consists of a ring gap of 0.002 m. For the V-flame configuration the same burner body is used, but the bluff-body is removed and a stabilizing wire (d = 0.002 m) is installed symmetrically 10 mm above the nozzle (now d = 0.048 m) perpendicular to the light sheet. Here the turbulence grid determines the turbulence degree of the V-flame.

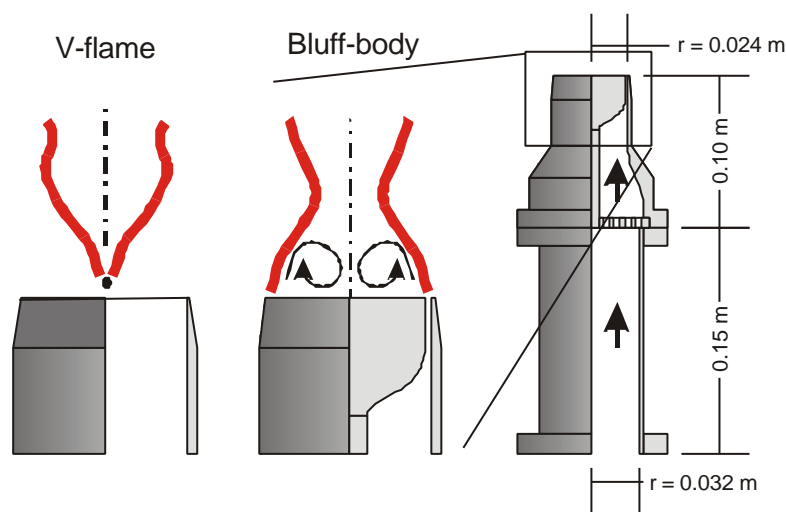Fig. 3:   Schematic of the burner body and the investigated burner heads V-flame (wire stabilized, d = 0.002 mm) and bluff-body configuration (d = 0.044 m).

4 RESULTS

4.1 Simultaneous temperature and velocity field

For both flames, measurements have been obtained in a height from 9 to 35 mm above the nozzle exit. For every operation point a series of at least 25 images is achieved.

To illustrate the applicability and expose the advantages of simultaneous FRS and PIV measurements, in Fig. 4 the vector field and the corresponding temperature field of two sequenced single shot images ($\Delta t \sim 1.5$s) at constant operation point (V-flame, $\phi = 0.7$, $v_{exit} = 0.9$ m/s), are exemplary presented.

The general flow direction is upward. Clearly visible is the v-shaped temperature structure of the flame being stabilized above the marked flame holder (semicircle). From that within ~2 mm the temperature ascends to full maximum. Note that, although the flame holder was hit by the laser beam, temperature measurements in direct neighborhood to this stabilization wire are possible from filtered Rayleigh scattering technique, which is impossible from conventional laser Rayleigh scattering
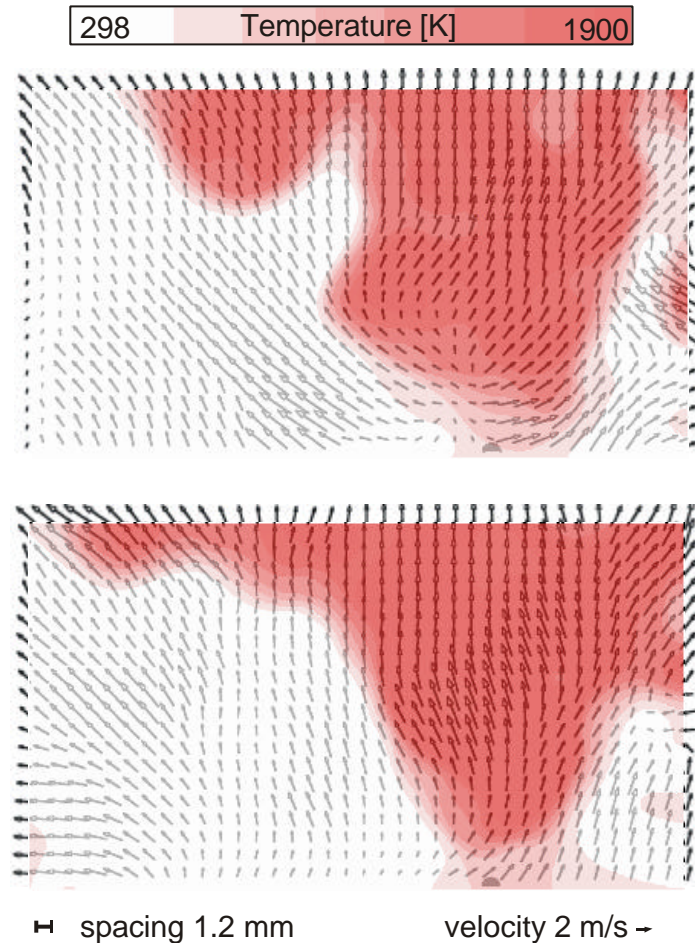

Fig. 4: Two exemplary images of the instantaneous temperature and velocity field of a V-flame. For reason of clarity vector separation is reduced to 1.2 mm. ($\phi = 0.7$, $v_{exit} = 0.90$ m/s)

A comparison of both data sets exposes the need for simultaneous measurements for turbulent flows. Already at this weak turbulence for a fixed position in the flame the local velocity and temperature conditions are changing rapidly. Flow field and flame shape are linked directly. The influence of vortices is visible (see Fig.4 upper image: slightly left from the wire and in the center of the image; lower image: half height, right edge). These transient large flow structures have huge influence of the flame front contour, being able to fold the flame front strongly and dislocate the reaction zone.

Note, that such correlated data is not achievable from separately obtained measurements. Only in a simultaneous determination, local velocity and strain can be connected directly to local flame structure (temperature profile, curvature, etc.). This direct spatial correlation is necessary to gain detailed information about the local flow $\leftrightarrow$ reaction interactions.

4.2 Influence of local strain rate e_{xy}

While large scaled eddies essentially influence the flame front contour (Fig. 4), the local shear strain is considered to play an important role by altering the flame reaction [Bradley (1992)]. This parameter can be obtained from the 2d velocity vector data locally. Then the strain rate distribution can be correlated with the temperature information from the simultaneously taken FRS measurements.

To give an example of such an evaluation, in Fig. 5 a single shot image of the velocity vector map (upper image) and the derived strain rate ε_{xy} distribution (lower image) of a highly turbulent flame (bluff-body burner, $\phi = 0.7$; $v_{exit} = 8.5$ m/s) is displayed.

The position of the bluff-body and the nozzle is marked below the images. Also plotted is flame front as black line. This contour line is obtained from the corresponding FRS measurements by the setting a threshold at 1200 K and indicates the location of the reaction zone.

The instantaneous velocity field shows the recirculating flow on the left side of the flame. Noticeable are the high absolute values of the strain rates directly on the fresh gas side and on the burnt side of the flame front. Here, the sign orientation of the strain is reciprocal. In the recirculation zone negative, in the free jet positive values are present. The gradient between these two extrema is maximal at height of 10 mm and descends slightly till the height of 30 mm.

Somewhere between the extrema of ε_{xy} the flame front is stabilized. The progression of the flame contour fits well to the border line marked by the shear strain maximum, resp. minimum. The same curvature is visible from the flame contour line as from the strain rate border line, showing small corresponding folding waves of ~8 mm length).

For better visualization of the shear strain rate near the flame front a magnification of the horizontal profile plot (height 10 mm) is drawn in Fig. 6. Coming from the free jet (r > 23 mm), within two millimeters the strain rate drops from nearly +5000 1/s to -5000 1/s at r ~ 21 mm. Surprisingly the flame front is not located at zero level, but stabilizes itself somewhere nearer (r ~ 21.5 mm) to the hot recirculation zone with negative strain rate, which is typically for the bluff-burner at these turbulence conditions. At this point also the highest gradient of ε_{xy} exists. Although not done in the current work, it might be interesting to compare such findings with theories of flame stabilization.
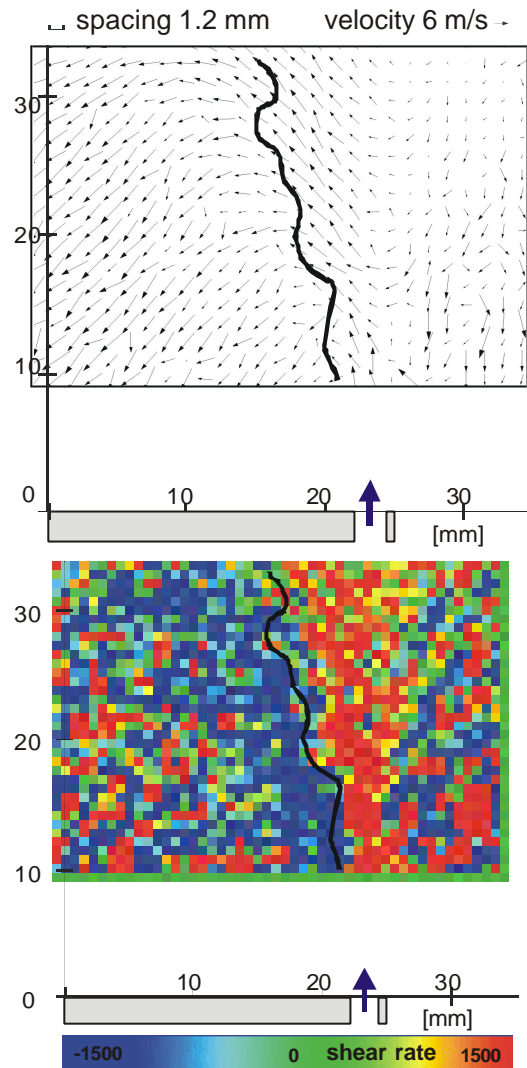

Fig. 5: Single shot image of velocity (upper image) and shear strain ε_{xy} of a recirculation flame (lower image). The flame front, obtained at 1200 K from simultaneous temperature measurements (FRS) is indicated.
(bluff-body burner; $\phi = 0.7$; $v_{exit} = 8.5$ m/s)

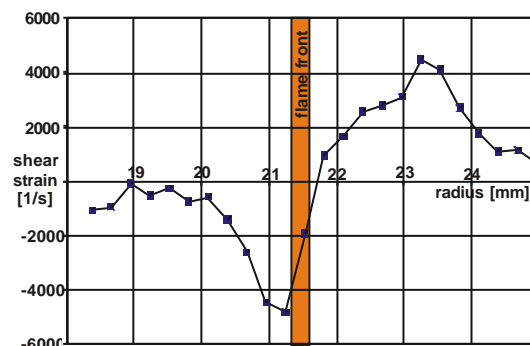Fig. 6: Strain rate ε_{xy} profile at 10 mm from Fig. 5. Marked the position of the flame front

	$\bar{v}$ [m/s]	v'_{ms} [m/s]	T_u [-]	ν [m²/s]	a_T [1/s]	ε_{xy} [1/s]
PIV						
cold	4.89	**0.37**	0.08	0.899	**197.5**	**6102**
hot	7.80	**0.86**	0.11	6.973	**138.5**	**1026**
non-conditioned						
(ν 298 K)	7.02	**1.49**	0.21	0.899	**1592.6**	**2514**
(ν 1800 K)	7.02	**1.49**	0.21	6.973	**315.8**	**2514**
LDV						
non-conditioned						
(ν 298 K)	7.32	**1.91**	0.26	0.899	**2311.4**	-
(ν 1800 K)	7.32	**1.91**	0.26	6.973	**458.3**	-

Table 1: Exemplary result of temperature conditioned/non-conditioned evaluation of strain factor a_T and local strain ε_{xy} obtained for a time series at one fixed location in the flame brush. (bluff-body burner, $v_{exit} = 8.48$ m/s, h = 20 mm ; the kinematic viscosity ν is calculated for cold (298 K), hot.

4.3 Comparison between direct and time averaged turbulence intensity and local strain rates

For the characterization of turbulent flames, the measurement of the local mean velocity, velocity fluctuation and of the local strain rate of the flow is of considerable interest. The latter quantity determines especially the alteration of the local transport and reaction processes inside the reaction zone. From simultaneous planar velocity and temperature field measurements two advantages are expected here. On the one hand now a separated evaluation of the mean velocity and rms-velocity fluctuation values for burnt or unburnt part of the flame is possible in contrast to non-conditioned time averaged determination with standard LDV measurements. On the other hand, in order to determine local strain rates, instantaneous spatial velocity gradients can be measured directly. Up to now, only a time averaged estimation of the local strain rate has been possible, using for instance LDV data. Here, the mean turbulent strain rate a_T commonly is determined from the rms-velocity fluctuation of the flow and the Taylor length scale l_T [Bradley (1992)] with

$$a_T = \frac{v'_{ms}}{l_T} = \frac{v'_{ms}}{6.35 \cdot \dfrac{L_x}{Re_T^{0.5}}} = \frac{v'_{ms}{}^{1.5} \cdot}{6.35 \cdot L_x{}^{0.5} \cdot \nu^{0.5}} \qquad (8)$$

where l_T is calculated from the turbulent Reynolds number $Re_T = (v' \, L_x)/\nu$. The macro length scale L_X, which marks the scale of the largest eddies in the flow is considered to 2 mm (ring gap width). ν is the kinematic viscosity of the gas sample.

In the present work comparisons have been done between time-averaged non-conditioned data from LDV and PIV measurements concerning the mean velocity, the velocity fluctuation and the strain rate a_T. Additionally, a comparison between conditioned and non-conditioned data from instantaneous PIV data in correlation to the instantaneous FRS data has been done for these quantities and also for the local shear strain rate ε_{xy}.

For that, one point of interest has been chosen in the flame brush of a bluff-body stabilized flame ($\phi = 0.7$, $v_{exit} = 8.48$ m/s, h = 20 mm, r = 20 mm) is exemplary picked out. From a series of 30 the average velocity $\bar{v}$ and the corresponding root mean square value of the fluctuation v' is calculated at this fixed point. Additionally from the temperature measurements a conditioning of v and v' is done. Velocities with temperatures above 1200 K are regarded to be from hot burnt gas, below 1200 K to belong to cold unburnt gas. Exemplary results are given in Table 1 and graphically illustrated in Fig. 7.

While the non-conditioned evaluation produces an average velocity with high fluctuation for both measurement techniques (PIV & LDV), the temperature conditioned determination divides the measured velocity into two parts. One part with low mean velocity belongs to cold, while the other part with high velocities is significantly correlated to hot burnt gas. This indicates a strong bi-modal distribution in the flame brush, which results from the strong density increase in the combustion process. The fluctuation v'_{ms} for the hot region is higher than for
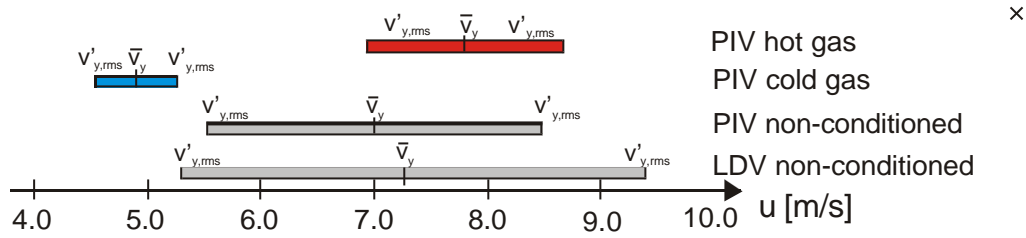
Fig.7: Average velocity and rms-values of the fluctuation obtained for a time series of data at one fixed location in the flame brush (bluff-body burner, $h = 20$ mm, $r = 20$ mm, $\phi = 0.7$, $v_{exit} = 8.5$ m/s)

the cold one but still smaller than those, deduced from non-conditioned measurements. From the latter ones significantly overestimated values are determined.

Analogously a conditioned determination of a_T can be achieved for simultaneous FRS-PIV data. For reasons of comparability for non-conditioned evaluation two viscosities are inserted into eq. (8): One for cold and unburnt gas at 298 K and one for the burnt gas (1800 K). The gas composition at T itself is considered from calculations of the laminar flame structure (CHEMKIN calculations). For the conditioned evaluation only the cold resp. the hot value is regarded. From eq. (8) it is obvious, that a_T is directly linked to v'_{rms}. Consequently from the for non-conditioned evaluation significantly overestimated values of v'_{rms}, now strongly biased numbers of the strain factor a_T are calculated. From conditioned evaluation much smaller values result (compare Fig. 8).

For directly determined strain rate values $|\epsilon_{xy}|$ again a separation in small hot and large cold gas values is achievable by conditioning to temperature (compare Fig. 9). Here, the non-conditioned values are located between those two conditioned levels, which seems quite reasonable in contrast to the indirectly determined strain rate a_T. But the trend of separation in one higher cold and one lower hot strain rate value is given for conditioned direct (ϵ_{xy}) as same as for conditioned time averaged (a_T) determination. Note the absolute value of a_T depends strongly on L_x, which is only estimated here.

Thus for nearly bi-modal distributions of velocity, as they are given in the flame brush of premixed flames, a non-conditioned evaluation of v'_{rms} and from that a_T gives the false impression of too high turbulent shear strain rates. If a conditioned evaluation is proceeded, much lower strain rates a_T are obtained, which fit well to the directly determined local shear strain ϵ_{xy}.
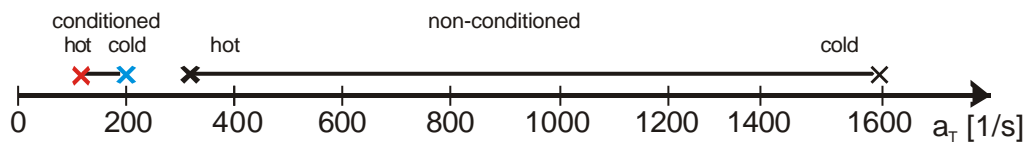

Fig. 8: From Fig. 7 calculated strain factors a_T for temperature conditioned or non-conditioned evaluation (PIV data only).
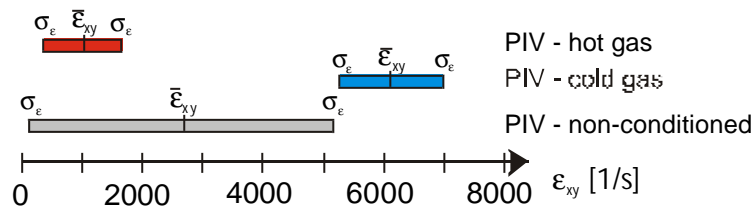

Fig. 9: Directly determined local strain ϵ_{xy} obtained for a time series of data at one fixed location in the flame brush. (bluff-body burner, $h = 20$ mm, $p = 0.7$, $v_{exit} = 8.48$ m/s)

5 CONCLUSION

Exemplary measurements by simultaneous application of FRS and PIV on a turbulent V-flame and a bluff-body burner are presented. These new combination of measurement techniques enables the simultaneous determination of the instantaneous velocity and temperature field.

From that, the influence of the velocity field on the flame shape is directly visible. Local flow parameters can be determined directly (e.g., strain rate ε_{xy}, vorticity) and can be correlated to the local flame parameters (e.g., temperature, curvature). Thus from the simultaneously obtained data sets more detailed information about the flow $\leftrightarrow$ flame interaction of turbulent flames can be gathered.

For the characterization of flames, a separation of the obtained flow parameters into hot and cold gas values is now possible and is shown to be reasonable. By non-conditioned determination (e.g., from LDV in flames) to high values for v'_{ms} and correspondingly of the mean turbulent strain rate a_T are produced in the flame brush. This systematic error is caused by the local swaying flame front and the huge density difference between the cold gas flow before front and the hot gas flow behind it. Simultaneous planar velocity and temperature measurements have the potential to avoid this significant bias.

REFERENCES

Bradley, D. (1992). How fast can we burn. Twenty-Fourth Symposium (International) on Combustion, The Combustion Institute, Pittsburgh, PA.

Carter, C. D., J. M. Donbar and J. F. Driscoll (1998). "Simultaneous CH planar laser-induced fluorescence and particle imaging velocimetry in turbulent non-premixed flames." Applied Physics B **66**: 129-132.

Chu, B. (1991). Laser Light Scattering. Boston, USA, Academic Press.

Dinkelacker, F., et al. (1998). Structure of locally quenched highly turbulent lean premixed flames. Twenty-Seventh Symposium (International) on Combustion, Boulder, Colorado, USA, The Combustion Institute, Pittsburgh, PA.

Duarte, D., P. Ferrao and M. V. Heitor (1995). Flame structure characterization based on Rayleigh thermometry and two-point laser-Doppler measurements. Developments in Laser Techniques and Fluid Mechanics. J. R. e. a. Adrian. Berlin, Springer.

Elliott, G., S. and M. Samimy (1996). "Rayleigh Scattering Technique for Simultaneous Measurements of Velocity and Thermodynamic Properties." American Institute of Aeronautics and Astronautics **34**(11): 2346-2352.

Forkey, J. N. (1996). Development and Demonstration of Filtered Rayleigh Scattering - A Laser based Flow Diagnostic for Planar Measurement of Velocity, Temperature and Pressure. Mechanical and Aerospace Engineering. Princeton, N.J., Princeton University**:** 297.

Forkey, J. N., W. R. Lempert and R. B. Miles (1997). "Corrected and calibrated I2 absorption model at frequency-doubled Nd:YAG laser wavelengths." Applied Optics **36**(27): 6729-6738.

Frank, J. H., A. M. Kalt and R. W. Bilger (1999). "Measurements of conditional velocities in turbulent premixed flames by simultaneous OH PLIF and PIV." Combustion and Flame **116**(01-02): 220-232.

Göttgens, J., F. Mauss and N. Peters (1992). Analytic Approximations of the burning velocities and flame Thickness of lean Hydrogen, methane, ethylene, ethen, acetylene and propane flames. Twenty-Fourth Symposium (International) on Combustion, The Combustion Institute, Pittsburgh, PA.

Hofman, D., K.-U. Münch and A. Leipertz (1996). "Two-dimensional temperature determination in sooting flames by filtered Rayleigh scattering." Optics Letters: 525-527.

IoP (1997). Special Issue: Particle image velocimetry. Measurement Science and Technology, Institute of Physics Publishing. **8**.

Leipertz, A., G. Kowalewski and S. Kampmann (1992). Measurement of Gas Temperature and Temperature Structures in Premixed Flames by Using Laser Rayleigh Techniques. New York, Am. Institute of Physics.

Mansour, M. S., N. Peters and Y.-C. Chen (1998). Investigation of Scalar Mixing in the Thin Reaction Zones Regime Using a Simultaneous CH-LIF/Rayleigh Laser Technique. Twenty-Seventh Symposium (International) on Combustion, Boulder, Colorado, USA, The Combustion Institute, Pittsburgh, PA.

Most, D., F. Dinkelacker and A. Leipertz (2000). "Combined determination of temperature and velocity by simultaneous application of filtered Rayleigh scattering and particle image velocimetry." Optics Letters **submitted**.

Most, D. and A. Leipertz (1999). Filtered Rayleigh scattering thermometry - calibration of cross section factors. The Combustion Institute - Joint meeting of the British, German and French Section, Nancy, The Combustion Institute.

Most, D., A. Soika, F. Dinkelacker and A. Leipertz (1999). Simultaneous planar OH and temperature measurements for the detection of lifted reaction zones in premixed bluff-body stabilized flames. Developments in Laser Techniques and Fluid Mechanics. R. J. Adrian, et al. Berlin New York, Springer.

O'Young, F. and R. W. Bilger (1997). "Scalar gradient and related quantities in turbulent premixed flames." Combustion and Flame **109**: 682-700.

Peters, N. (1986). Laminar Flamelet Concepts in Turbulent Combustion. Twenty-First Symposium (International) on Combustion, The Combustion Institute, Pittsburgh, PA.

Poinsot, T., D. Veynante and S. Candel (1993). Diagrams of premixed turbulent combustion based on direct simulation. Twenty-Third Symposium (International) on Combustion, The Combustion Institute, Pittsburgh, PA.

Raffel, M., C. Willert and J. Kompenhans (1998). Particle Image Velocimetry. Berlin, Springer.

Rehm, J. E. and N. T. Clemens (1998). The Relationship between Vorticity/Strain and Reaction Zone Structure in Turbulent Non-Premixed Jet Flames. Twenty-Seventh Symposium (International) on Combustion, Boulder, Colorado, USA, The Combustion Institute, Pittsburgh, PA.

Roberts, W., L., J. Driscoll, F., M. C. Drake and J. Ratcliffe, W. (1992). OH Fluorescence Images of the Quenching of a Premixed Flame during an Interaction with a Vortex. Twenty-Fourth Symposium (International) on Combustion, The Combustion Institute, Pittsburgh, PA.

Soika, A., F. Dinkelacker and A. Leipertz (1998). Measurement of the resolved flame structure of turbulent premixed flames with constant Reynolds number and varied stoichiometry. Twenty-Seventh Symposium (International) on Combustion, Boulder, Colorado, USA, The Combustion Institute, Pittsburgh, PA.

Stevens, E. J., K. N. C. Bray and B. Lecordier (1998). Velocity and Scalar Statistics for Premixed Turbulent Stagnation Flames Using PIV. Twenty-Seventh Symposium (International) on Combustion, Boulder, Colorado, USA, The Combustion Institute, Pittsburgh, PA.